Performance Evaluation of Solar-Assisted Heating System for Drying Multi-Commodity Crops

Jonathan H. Perez[1*], Jude Andrea Eve Maternal[1, 3], Antonio Abdu Sami Magomnang[2], Marvin Rosales[2] and Reyvencer Reyes[2]
[1]College of Science and Mathematics
[2]College of Engineering and Architecture
[3]Northern Mindanao Food Innovation Center
University of Science and Technology of Southern Philippines – Cagayan de Oro
Cagayan de Oro City, 9000 Philippines
[*]*jo.nsyc@gmail.com*

Date received: December 4, 2023
Revision accepted: September 11, 2024

Abstract

Energy scarcity and food security are significant global challenges worsened by post-harvest losses and alarming hunger statistics, spurring agriculturists, food scientists, engineers, and decision-makers to promote global food security. Solar drying has gained recognition as a high-quality, eco-friendly method for food preservation. This study investigates a newly designed hybridized solar dryer equipped with solar reflectors for drying the most produced commodities in Northern Mindanao. The experiment considers three factors: loading density, slice thickness and drying tray location across three fruit samples- green Cardaba bananas, partially ripe mangoes and ripe pineapples. The experiment utilized the complete randomized design with three replications. The samples were procured locally, peeled, washed, and cut into 6 mm and 10 mm thick slices. Drying was conducted at two different loading densities of 53 and 107 g/100 cm^2 from approximately 9:00 AM to 3:00 PM. Various drying parameters were monitored, including solar insolation, temperature distribution in the drying chamber, moisture characteristics curves and drying rate curves. Results showed initial moisture contents of 160 -190 % for bananas, 160 -270 % for mangoes, and 400-590 % for pineapples. Solar insolation peaked at approximately 800 W/m^2 between 11:00 AM and 1:00 PM. Higher drying rates were observed for samples in the top layer, with varying rates due to changes in solar insolation. The new dryer design effectively accommodates both slice thicknesses for all three commodities, making it a suitable option for communities in Northern Mindanao and nearby regions, with potential for extended use during nights or cloudy seasons.

***Keywords**:* drying characteristics, drying rate, multi commodity crops, solar drying, solar heater

---

1. Introduction

Northern Mindanao is strategically located in the southern part of the Philippines' resource-rich island of Mindanao. It is a highly diversified region known for its quality of life and sustained economic growth. Dubbed the country's food basket, it produces a significant quantity of agricultural products, including vegetables, rice, corn, sugar, coffee, and fruits like pineapple and banana. According to the Philippine Statistics Authority in 2020, total production of selected major crops in Northern Mindanao reached 3.377 million metric tons (MT) in the first quarter of 2020 (PSAX-SR-2020-13). However, poor post-harvest storage and processing have resulted in considerable losses. Mopera (2016) reported that post-harvest losses for both bananas and pineapples in the Philippines range from 5-33%. In Northern Mindanao, there is a lack of numerical data on post-harvest losses in pineapples, but a report by Gerance (2023) indicated that losses of queen pineapples in Camarines Norte reached 47.81%. Factors contributing to these losses include mechanical damage, premature ripening, weight loss, and rotting in bananas, as well as latex damage and cracking disease in mangoes. Additionally, topography, distance from farms, and poor handling practices contribute to these losses. Suggested solutions to mitigate post-harvest losses include the use of ethylene absorbents, careful handling, and treatments such as alum and hot water for mangoes (Mopera, 2016).

Solar energy is a limitless and renewable resource. Consequently, power industries in Northern Mindanao are investing in solar farms to generate electricity for manufacturing industries and residential homes (Jerusalem, 2021; CDO Encyclopedia, n.d). Given its geographical location, Northern Mindanao receives abundant solar energy, which can be harnessed for drying various agricultural products, including mangoes, pineapples, and bananas, thus addressing the issue of post-harvest losses. Drying is a widely used technology for preserving fruits and vegetables, wherein moisture is removed from the food product through heat application from solar radiation (Salazar-Camacho *et al*., 2022). The removal of moisture ensures product stability and minimizes chemical and physical changes. The energy needed in the dryer depends on the materials being dried and the technology employed (Pirasteh *et al*., 2014).

Agricultural products such as mango, banana and pineapple are harvested in volumes and the rate of immediate consumption from the community has a wide disparity. Due to the highly perishable nature of these commodities, if left unprocessed, these products spoil easily. Mangoes, pineapples, and bananas are soft fruits that can easily sustain interior damage when handled improperly or subjected to excessive force during post-harvest handling and storage, leading to rapid deterioration when exposed to air for extended periods. Furthermore, these commodities are also considered climacteric fruits (Asrey *et al*., 2023; Zhang *et al*., 2017). Climacteric fruits often continue to ripen even after being separated from the plant. They are also distinguished by a high rate of respiration and ethylene emission. The high rate of respiration and ethylene emission resulted to the faster softening of the fruit (Pech *et al*., 2008). Thus, resulting to significant wastage amplifying the losses due to poor postharvest handling. Hence, reducing the post-harvest losses through drying offers considerable solution by giving farmer communities opportunity to improve their income and quality of life.

Recently, solar drying has gained recognition as a cost-effective drying method compared to other technologies. It is sustainable because the utilization of renewable solar energy is free. In rural communities and areas with limited electricity supply, solar drying can facilitate crop drying and food processing (Sacilik, 2007). In addition, Mohammed *et al.* (2020) reported that fruits dried using the conventional solar dryer exhibit higher organoleptic qualities. Recommended drying temperatures of mangoes, pineapple and banana ranged from 40-80 ^{o}C (Yan *et al*., 2008; Rani and Punam, 2022).

Several solar drying technologies have been developed for drying of agricultural commodities (Mustayen *et al*., 2014). Various designs and sizes have been developed to suit specific purposes (Mustayen *et al*., 2014; Mohana *et al*., 2020). One type of solar dryer is the concentrated solar dryer, which includes models such as linear Fresnel reflectors (FLR), parabolic trough collectors (PTC), solar towers, and solar disks—commonly used solar concentrator technologies (Liang *et al*., 2021; Xiao *et al*., 2021).

This study experimentally investigates the drying of green Cardaba bananas, pineapples, and mangoes using a hybridized solar dryer equipped with solar reflectors and a backup solar cell. The aim is to assess the performance and efficiency of the hybridized solar dryer in drying these three commodities under the recommended drying temperature levels.

2. Methodology

2.1 Preparation of Raw Materials for Drying

The fruit samples, including whole pineapples, green bananas and mangoes were procured from Cogon Market, Cagayan de Oro City and transported to the Northern Mindanao Food Innovation Center (NMFIC) at the University of Science and Technology of Southern Philippines, Cagayan de Oro City for processing.

The preparation of the samples for drying followed a detailed procedure. For the experiments, the thickness of the samples was standardized at 6 mm and 10 mm, respectively. Previous studies on the drying characteristics of various products have utilized a similar range of sample thicknesses (Mugodo and Workneh, 2021; Dereje *et al.*, 2020; Elhesain *et al.*, 2023; Espinoza *et al.*, 2023; Gilago *et al.*, 2023; Gilago and Chandramohan, 2023; Phyu *et al.*, 2024; Thao *et al.*, 2024). The process flow of the methodology employed is illustrated in Figure 1.

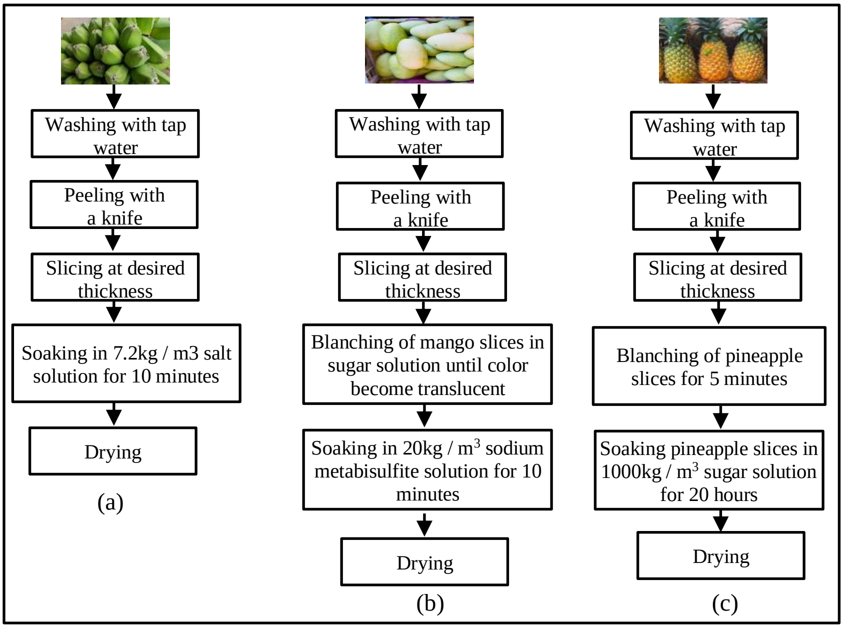

Figure. 1. Flow diagram of the drying process for the three commodities: Green Cardaba Banana (a); Partially Ripe Mango (b); Ripe Pineapple (c)

2.1.1 Banana

Green Cardaba banana samples were selected for this study. The bananas were washed with clean water, and the peel was carefully removed using a sharp knife. The triangular ends of the peeled bananas were sliced off and discarded. To prevent browning, the peeled bananas were soaked in water before being sliced to the desired thickness.

2.1.2 Mango

Mature and partially ripe mangoes were selected for the study. The mangoes were washed with tap water and peeled using a sharp kitchen knife. After peeling, the mango samples were soaked in tap water for further processing. They were then sliced longitudinally and cut to the desired thickness. The sliced samples were blanched for 30 minutes until their color became translucent. After blanching, the samples were soaked in a solution of sugar at a 1:1 ratio by weight to the samples in 1 liter of water for 20 hours.

2.1.3 Pineapple

Mature and partially ripe pineapples were selected for the study. The pineapples were washed with tap water and peeled using a sharp kitchen knife. After peeling, the eyes were removed, as they are not edible. The cleaned pineapple samples were then soaked in tap water for further processing. The peeled pineapples were sliced to the desired thickness and size. The sliced samples were blanched for 5 minutes until they became translucent. After blanching, the samples were soaked in a solution of sugar at a 1:1 ratio by weight to the samples in 1 liter of water for 20 hours.

2.2 Solar Heater Dryer

A comparison of the professional solar oven made by Lytefire Inc. in Finland and the schematic diagram of the fabricated assembly of the solar dryer-roaster is shown in Figure 2. The solar dryer-roaster features a cluster of reflectors arranged in a curved design to concentrate the intensity of solar radiation onto the roasting and drying chamber of the machine. The assembly design was based on the Lytefire model (Lytefire Pro, Lytefire Inc., Finland), with some modifications. In the present modified design, a backup electric heater was included to compensate for instances when solar insolation is inadequate for drying operations. A photovoltaic cell connected to a 12-volt battery powers the electric heater. This backup system is designed to enhance heat production when solar energy collected from the reflectors is insufficient to reach the desired temperature.

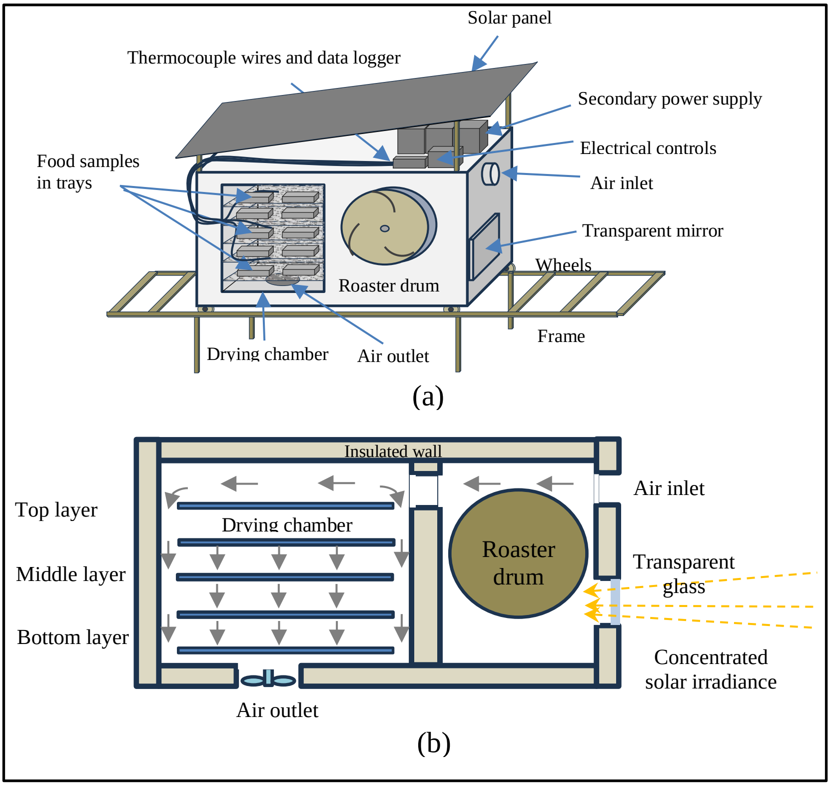

Figure 2. Comparative diagram of the solar dryer-roaster: Schematic diagram of the solar dryer-roaster assembly with backup solar panel without the solar reflector used in the drying and roasting experiment (a); Schematic diagram of the heat and air flow inside the heating chamber (b)

This feature is particularly beneficial during times when cloud cover exceeds 50%, blocking solar insolation. However, during the data collection, the solar panel was not yet operational. The solar reflectors are made up of glass mirrors with dimensions of 60 cm in length and 19 cm in width. Three layers of solar reflectors with 19 pieces in each row. The mirrors are attached to the metal frame assembly with the use of a super glue. The row of mirrors is positioned 270 cm away from the drying/roasting chamber. The base frame of the assembled concentrated solar dryer-roaster is equipped with two wheels to change the position reflectors as the sun changes its position throughout the day. Similarly, the drying and roasting chamber is also equipped with four base wheels and a guide rack to adjust the aperture of the incident solar radiation. Throughout the day, the heat generated from the incident solar radiation reflects to the drying and roasting chamber through the reflecting mirrors thus increasing the temperature appropriate for the roasting and drying operation. A rectangular opening, 25 cm by 31 cm, in the drying/roasting chamber covered with a clear glass allows the concentrated heat from the incident radiation to pass though and increase the temperature in the chamber. The dryer/roaster assembly has a width, length and height of 63, 110, and 80 cm, respectively.

2.3 Drying Experiments

The present experiment examines three different factors: loading density, slice thickness and drying tray location for all three fruit samples. All experiments were designed using a completely randomized design with three replications. The loading densities studied were 53 g/100 cm^2 and 107 g/100 cm^2. Additionally, the drying tray locations were evaluated in three different tiers within the drying chamber: the bottom, middle and top layers. Furthermore, two slice thicknesses of 6mm and 10 mm were utilized.

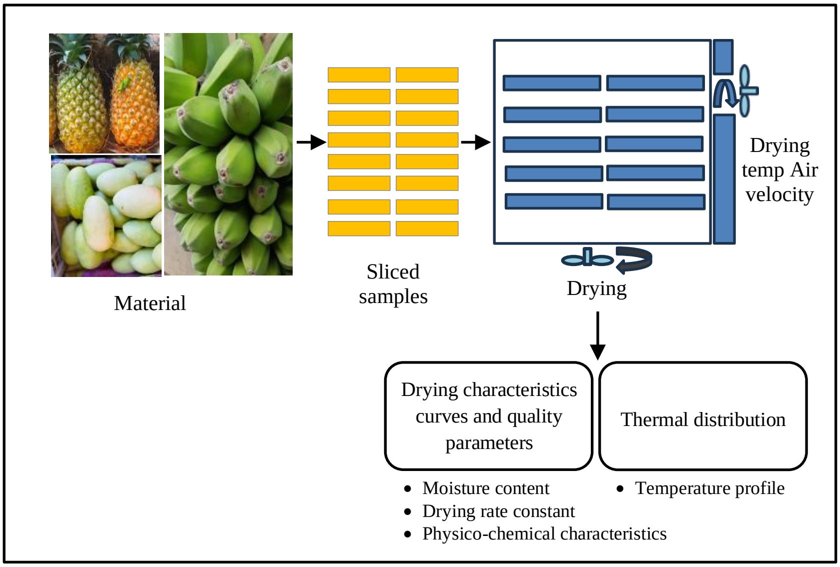

Figure 3. Schematic diagram used in the experimental set-up indicating the parameters monitored during the conduct of the experiment

The drying experiments for the three fruit samples were conducted to assess their drying characteristics. Figure 3 shows the schematic diagram used during the experiment. Pre-treated fruit sample slices were evenly scattered in prefabricated small stainless steel wire mesh trays and loaded in the drying chamber. The samples were dried for a designated duration until moisture equilibrium was reached. Moisture loss during drying was monitored by determining the weight loss of the samples at 15-minute intervals for the first hour and every 30 minutes thereafter. Changes in weight were measured using an electronic top-loading balance (JK-EB-502N, JKI China).

The different samples in the drying experiment were loaded into three layers within the drying chamber: top, middle, and bottom. Throughout the duration of the drying process, the temperature of the chamber was monitored using Type K thermocouple wires to ascertain the temperature characteristics. The thermocouples and data logger were brand new and had an accuracy of ± 0.2°C. Before use, the devices were calibrated against a certified thermometer, ensuring that the difference between readings was less than 1%. The calibrated thermocouples were then installed in the drying chamber through a small opening in the door, positioned to monitor the temperatures at the top, middle, and bottom layers of the drying trays. This temperature monitoring process helps explain discrepancies in drying conditions among the samples subjected to the same temperature. After drying, representative samples were oven-dried to obtain their bone-dry mass. Subsequently, the moisture content of the samples was computed using the formula shown in Equation 1.

The changes in the moisture content and drying rate of the samples were monitored using the equations employed by other researchers (Tan *et al.*, 2006; Pekke *et al.*, 2013; Abd El-Wahhab *et al*., 2023).

$$MC = \frac{M_i - M_{dm}}{M_i} \tag{1}$$

where:

MC = *moisture content, wet weight basis (%)*
M_i = *instantaneous weight of the sample at any time t, (g)*
M_{dm} = *dry weight of sample computed based from the final moisture content of the sample (g)*

The drying rate of the different slices was computed using the formula in Equation 2:

$$\frac{dMC}{dt} = \frac{MC_{(t+\Delta t)} - MC_t}{\Delta t} \qquad (2)$$

where:

MC_t = *instantaneous moisture content, dryweight basis (%)*
$MC_{(t+\Delta t)}$ = *moisture content of the sample after drying time interval, t*

2.4 Solar Insolation Monitoring

Due to the geographical location of Cagayan de Oro, sudden changes in the weather during the day are often encountered. Thus, monitoring of the solar insolation characteristics was necessary. The rate of solar radiation was measured using a handheld digital data logging solar power meter (ISM410, RS PRO, India), which has an accuracy of $\pm 10\ W/m^2$. The pyranometer device measures both direct and diffuse solar irradiance. It was positioned near the setup to ensure exposure to the sun's radiation. Monitoring was conducted every 30 minutes until the completion of the experiment.

2.5 Statistical design and analysis

The experimental design follows a three-factor analysis, with loading density, thickness, and location as the factors. The slopes of the fitted regression lines on the drying rate curves were analyzed using analysis of variance (ANOVA) and Tukey's test to compare the means. Statistical analysis was performed on the slopes of all fitted regression lines from the three replications across all treatments. The General Linear Model for balanced ANOVA in Minitab 2018 (Minitab, 2021) was utilized for this analysis.

3. Results and Discussion

3.1 Solar Insolation and Temperature Characteristics

When designing a solar power system for agricultural and food processing, it is essential to assess the availability of sunlight at a specific site and time. Solar radiation is characterized by solar irradiance, which indicates the power per area at a given moment, and solar insolation, which represents the energy received per area over a certain duration. Solar irradiance is measured in kilowatts per square meter (kW/m^2) and varies throughout the day, reaching a maximum of around 1 kW/m² during peak sunlight hours and dropping to 0 kW/m² at night. Solar irradiance levels are significantly influenced by location and prevailing weather conditions, leading to daily variations. To obtain solar irradiance data, both global and direct radiation measurements are taken periodically using instruments such as pyranometers for global radiation and pyrheliometers for direct radiation.

The experiments were conducted from November 2021 to February 2022. During this period, the measured solar irradiation characteristics varied between 150 and 800 W/m², as shown in Figure 4. Early in the day, solar intensity is lower and gradually increases throughout the middle of the day. By around 9:00 to 10:00 AM, with minimal cloud cover, solar insolation readings increase from 600 to 800 W/m². However, between 1:00 to 2:00 PM, solar insolation gradually declines to about 180 W/m². These findings are consistent with the report by Rani and Punam (2022) on the drying of pineapple slices. This reduction in solar insolation is attributed to cloud buildup descending from the elevated grounds of the nearby province of Bukidnon and the elevated barangays of Cagayan de Oro down to Macajalar Bay. The cloud cover blocks solar insolation, causing a significant decrease in solar intensity. On days with clear weather and minimal cloud cover, a consistent and smoother solar insolation curve is observed, as shown in Figure 4b. On such days, solar insolation levels range from around 450 W/m² at 9:00 AM to nearly 800 W/m² at 3:00 PM. After this period, solar insolation diminishes, resulting in insufficient heat reflected into the drying chamber to maintain the necessary drying temperature. Consequently, drying of the samples typically ceases after this period.

The temperature fluctuations in the different layers inside the drying chamber are illustrated in Figure 5. Monitoring the temperature within the drying chamber is crucial, as the rate of moisture removal from the various commodities depends on temperature. The temperature profile in the drying chamber was recorded for the top, middle, and bottom layers and plotted alongside the ambient temperature. As seen in Figure 5, the desired temperature range of 60 to 75°C was achieved during the early hours of drying. However, after 12:00 or 1:00 PM, temperatures inside the chamber began to decrease due to cloud buildup, resulting in reduced solar insolation concentration.

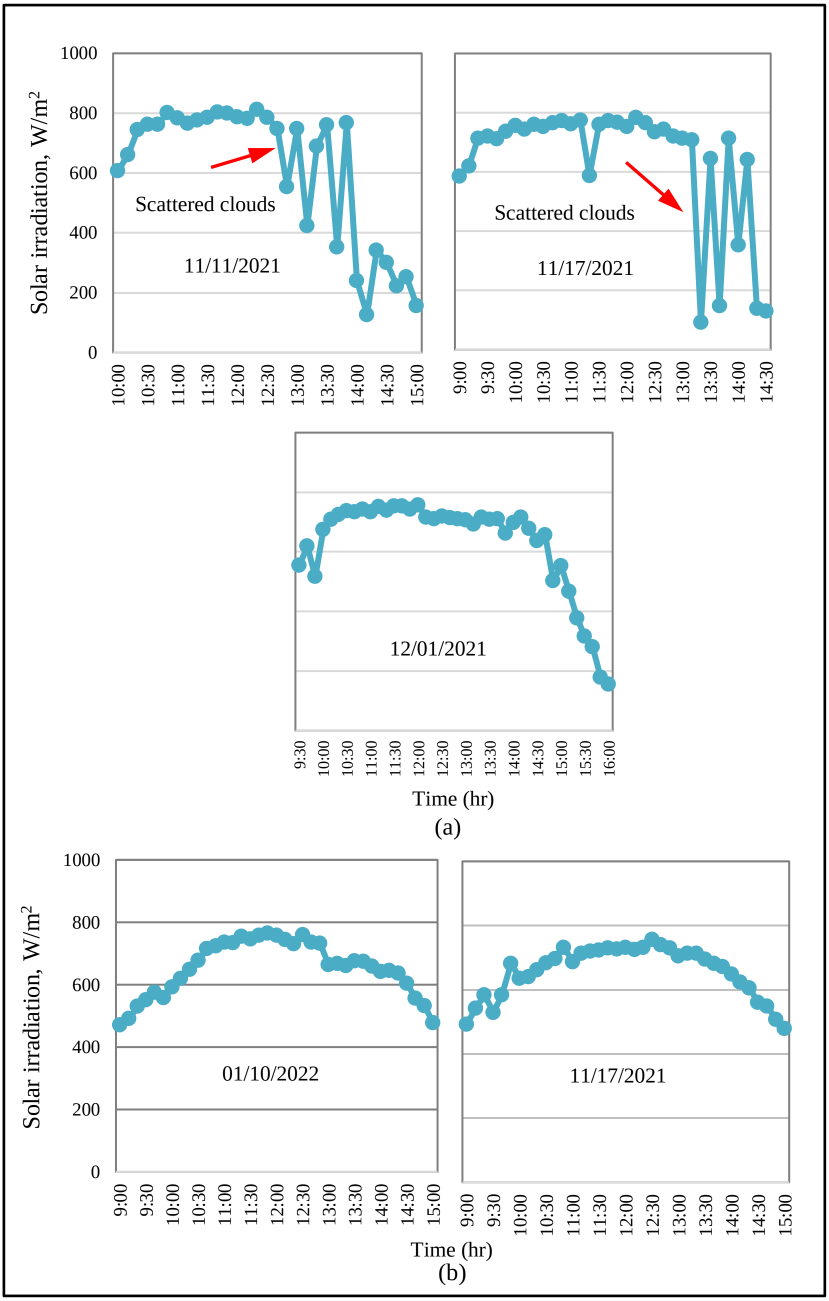

Figure 4. Variation of the solar radiation during a typical drying run: full sunny day in the morning with scattered cloud cover in the afternoon (a); full sunny day with no cloud cover in the afternoon (b)

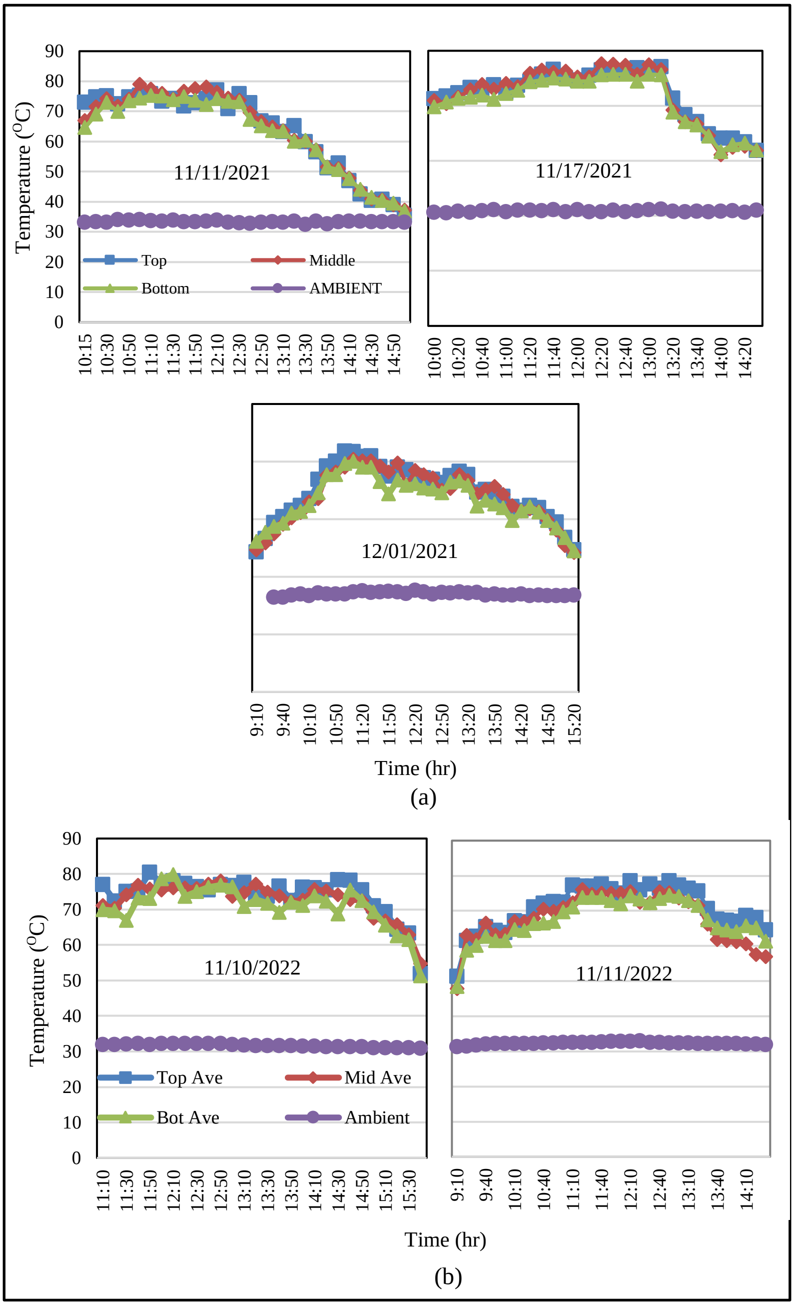

Figure 5. Temperature profile inside the dryer (top, middle and bottom) and the ambient temperature during a typical drying run of samples: full sunny day in the morning with scattered cloud cover in the afternoon (a); full sunny day with no cloud cover in the afternoon (b)

3.2 Fresh and Dried Samples

A comparison of the fresh and dried products for all three commodities is presented in Figure 6. Overall, all the dried products exhibited good quality in terms of color and texture, as determined by visual inspection at the end of the drying experiment.

Figure 6. Freshly prepared fruit slices on the left and dried samples on the right: fresh banana (a); dried banana (b); blanched and osmotically soaked mango (c); dried mango slices (d); blanched and osmotically soaked pineapple (e); dried pineapple slices (f)

3.3 Drying Characteristics Curves

The description of the drying characteristics of a product is a key method for determining the efficiency of dryers. This process involves assessing moisture removal and drying time to establish the drying characteristics. The drying characteristic curves are presented for a single commodity, with differing slice thicknesses also studied. Additionally, the sample slices were positioned in three different layers within the dryer to evaluate the dryer's performance relative to the drying characteristics of the various commodities. In the following section, the drying characteristics of each commodity will be presented.

3.3.1 Banana Slices

The drying characteristics of the banana slices are shown in Figure 7. Initially, the moisture content of the banana slices ranged from 160 to 190% g water/g dry matter under all drying conditions. The moisture content of the slices gradually decreased over the drying period, reducing from approximately 160-190% g water/g dry matter to around 70% g water/g dry matter after about 2-3 hours of drying.

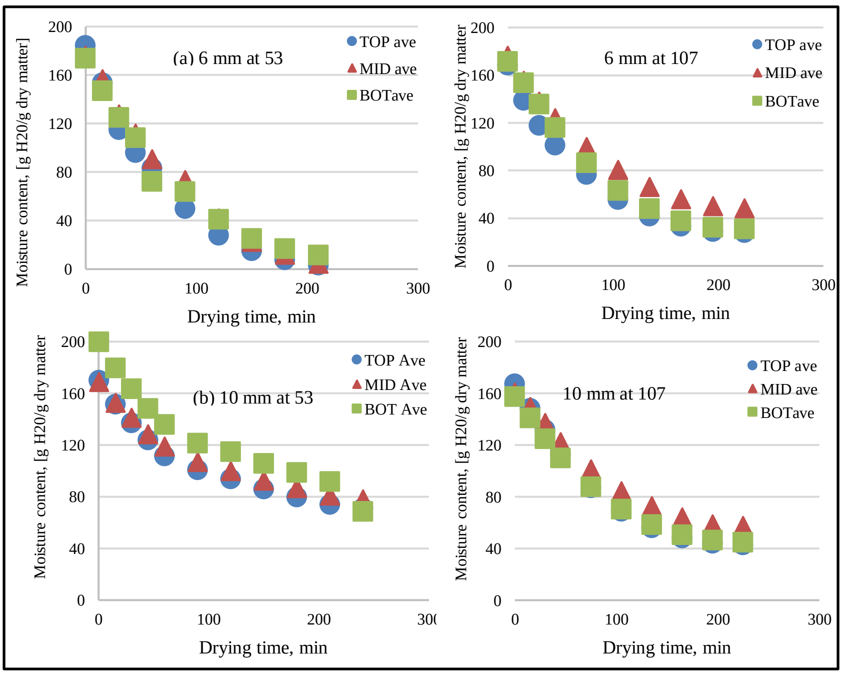

Figure 7. Drying characteristics of dried banana slices: 6 mm(a); 10 mm (b) [left figure is at loading density of 53 g/100 cm^2, right figure is at loading density of 107 g/100 cm^2.]

The drying curve for the banana slices was characterized by a progressive decrease in moisture over time, followed by stabilization at a constant moisture level. Similar findings were observed by Silva *et al.* (2022) during their study of Prata bananas. When comparing drying characteristics, samples dried in the top layer exhibited faster moisture removal compared to those positioned in the middle and bottom layers. This was expected, as temperatures in the top layer were slightly higher than those in the middle and bottom layers of the drying chamber.

3.3.2 Drying Rate Characteristics of Banana Slices

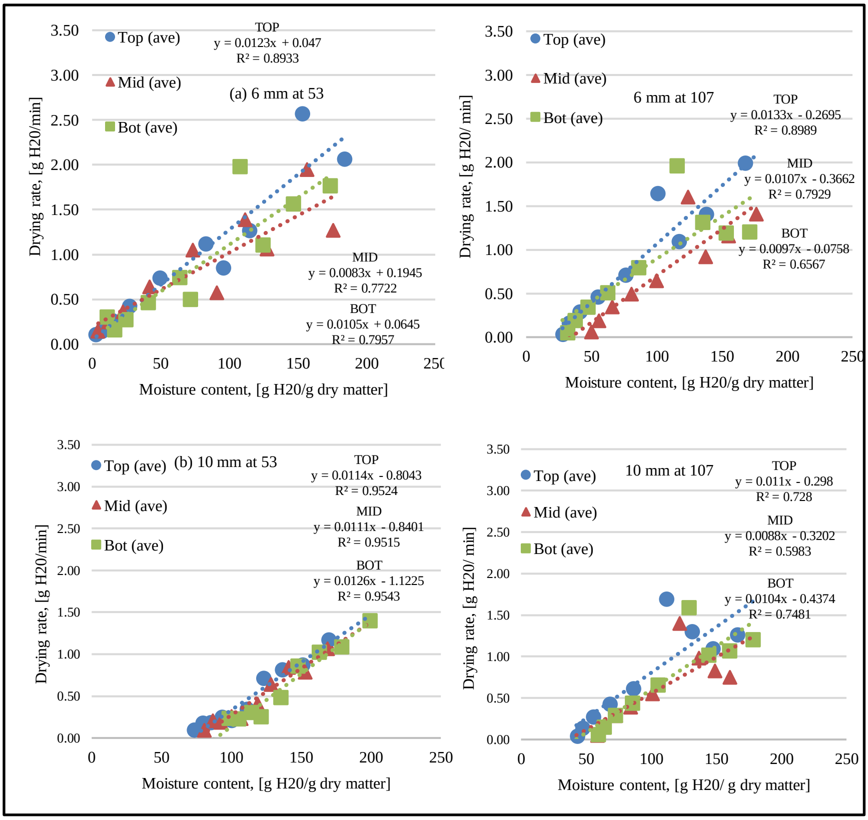

Figure 8. Drying rate characteristics of dried banana slices: 6 mm (a); 10 mm (b) [left figure is at loading density of 53 g/100 cm^2, right figure is at loading density of 107 g/100 cm^2.]

The drying rate characteristics of the banana slices are depicted in Figure 8. Evidently, the rate of moisture removal is faster in 6 mm slices compared to

10 mm slices, as indicated by the regression lines for all treatments studied. A linear regression was fitted to the drying rate curves to confirm that the drying rate follows a linear pattern, with the equations of the regression lines and the coefficient of determination (R^2) also presented. The slopes of the regression lines are significantly higher for the 6 mm slices than for the 10 mm slices. Moreover, the rate of moisture removal is greater in trays located in the top layer compared to those in the middle and bottom layers. Linear regression lines were fitted to the experimental data on the drying rate curves versus moisture content, as shown in Figure 8. The slope of the regression lines ranged from 0.0083 to 0.0133 across the two loading densities. Notably, the slope of the fitted regression lines supports the observation that the rate of moisture removal was higher in samples situated in the top layer compared to those in the middle and bottom layers. This phenomenon can be attributed to the higher temperatures in the top layer.

The effect of loading density is also evident in the drying rate characteristics of the samples. For sample thickness, no significant difference was found, with a P-value greater than 0.05. Conversely, the P-values for both location and loading density in all treatments, as shown in Table 1, were found to be less than 0.05. These values indicate a significant difference among the samples. Tukey's comparison of means revealed that the drying rate constants for samples located in the top layer are statistically different from those in both the middle and bottom layers.

Table 1. Analysis of variance on the value of the regression coefficient on the drying rate of banana slices

Source	DF	Adj SS	Adj MS	F-Value	P-Value
Location	2	0.000035	0.000018	12.364	0.00012
Thickness, mm	1	0.000000	0.000000	0.053	0.82006
Loading density, g/cm^2	1	0.000026	0.000026	18.340	0.00017
Error	30	0.000042	0.000001		
Lack-of-Fit	7	0.000021	0.000003	3.310	0.01382
Pure Error	23	0.000021	0.000001		
Total	34	0.000102			

3.3.3 Mango Slices

The drying characteristic curves for the mango slices are shown in Figure 9. The initial moisture content of the mango samples ranged from 160 to 270% g water/g dry matter across all samples with different thicknesses. This wide range of initial moisture content is attributed to the varying degrees of ripeness among the samples used in the experiment. In general, the rate of moisture removal is higher during the first two hours of drying compared to the subsequent minutes. This variation is due to changes in the intensity of solar insolation and temperature within the drying chamber. The drying characteristic curves for mango slices at 6 mm and 10 mm thicknesses with a loading density of 53 g/100 cm² appeared smoother and more consistent. In contrast, the drying characteristic curves for mango slices at 6 mm and 10 mm thicknesses with a loading density of 107 g/100 cm² exhibited slower progress and showed a noticeable dent in the drying curve. This dent indicates a stoppage in drying that lasted for several hours.

The interruption in drying occurred because the dryer was unavailable in the evening, leading to the discontinuation of the drying operation. The backup power source was not functional at that time, necessitating the halt in drying. Consequently, this discontinuation caused the moisture within the slices to equilibrate from the innermost portions to the surface of the slices.

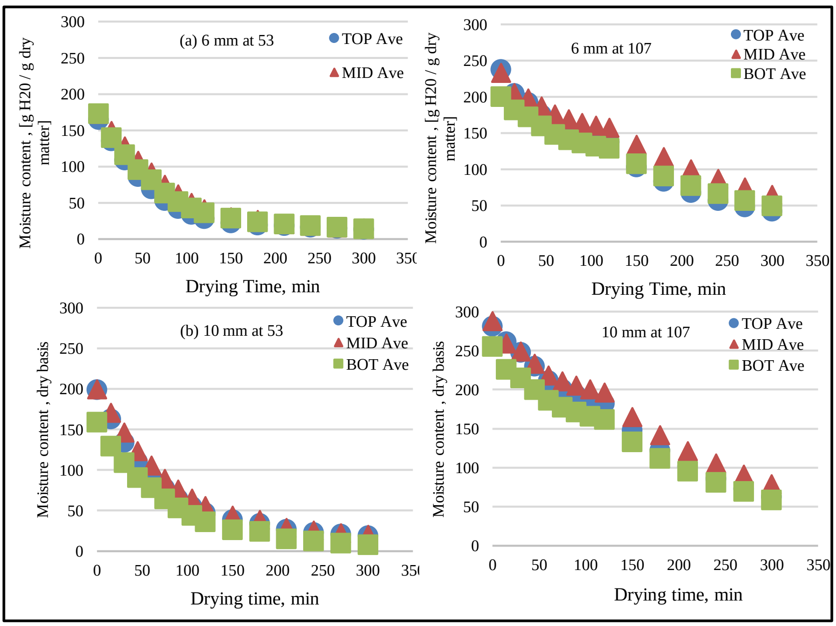

Figure 9. Drying characteristics of dried mango slices: 6 mm(a); 10 mm (b) [left figure is at loading density of 53 g/100 cm^2, right figure is at loading density of 107 g/100 cm^2.]

3.3.4 Drying Rate Characteristics of Mango Slices

The drying rate curves for the mango slices are shown in Figure 10. Linear regression lines were fitted to the drying rate curves to confirm that the drying rate follows a linear pattern. The drying rate curves for both the 6 mm and 10 mm slices at a loading density of 53 g/100 cm² exhibited two falling rate periods. The presence of these two falling rate periods can be attributed to the stoppage of the drying operation, which allows moisture within the mango slices to equilibrate. This stoppage permits the high concentration of moisture from the middle portion of the slices to migrate to the surface, where the moisture content is lower.

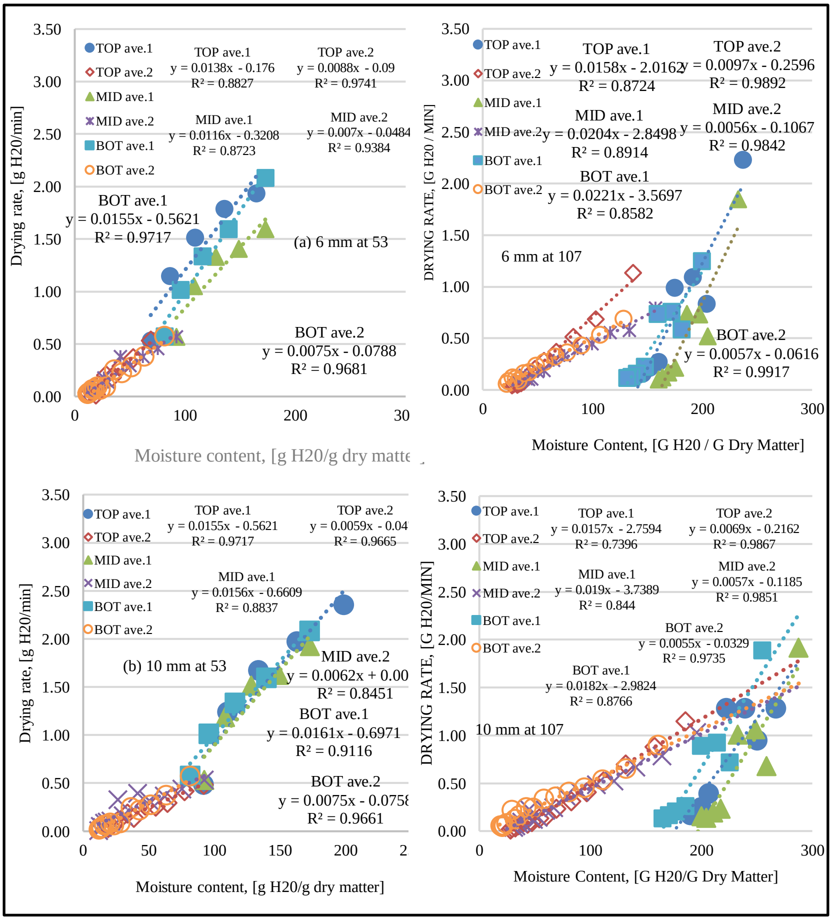

Figure 10. Drying rate characteristics of dried mango slices: 6 mm (a); 10 mm (b) [left figure is at loading density of 53 g/100 cm^2, right figure is at loading density of 107 g/100 cm^2.]

In the analysis of the drying rate, regression lines were fitted to both the first and second falling rate periods. The equations of the regression lines and the coefficient of determination (R^2) are also presented. The slope values of the fitted lines ranged from 0.0057 to 0.0204 across all treatments. The results of the statistical analysis on the slopes of the fitted lines are shown in Tables 2 and 3. In Table 2, the P-value under loading density was found to be less than 0.05, indicating a significant difference in drying rates between the two loading densities among the samples, while tray location and thickness did not show significant differences. However, the P-values for thickness and location in Table 3 were also found to be less than 0.05, indicating a significant difference. Samples dried in the top layer and 6 mm thick slices had a higher drying rate than those dried in the middle and bottom layers.

Table 2. Analysis of variance on the value of the regression coefficient on the first falling rate of mango slices

Source	DF	Adj SS	Adj MS	F-Value	P-Value
Location	2	0.000004	0.000002	0.170	0.84472
Loading density, g/cm2	1	0.000094	0.000094	8.212	0.00741
Thickness, mm	1	0.000001	0.000001	0.102	0.75150
Error	31	0.000356	0.000011		
Lack-of-Fit	7	0.000236	0.000034	6.721	0.00018
Pure Error	24	0.000120	0.000005		
Total	35	0.000456			

Table 3. Analysis of variance on the value of the regression coefficient on the second falling rate of mango slices

Source	DF	Adj SS	Adj MS	F-Value	P-Value
Location	2	0.000031	0.000015	11.508	0.00018
Loading density, g/cm2	1	0.000000	0.000000	0.226	0.63773
Thickness, mm	1	0.000011	0.000011	8.224	0.00737
Error	31	0.000041	0.000001		
Lack-of-Fit	7	0.000019	0.000003	3.016	0.02019
Pure Error	24	0.000022	0.000001		
Total	35	0.000084			

3.3.5 Pineapple Slices

The drying characteristics of the pineapple product are shown in Figures 11 and 12. The initial moisture content of the pineapple slices ranges from approximately 400 to 590 g water/g dry matter. This variation is likely due to differences in the degree of ripeness of the pineapple slices. Comparison of the drying curves for the various tray locations inside the drying chamber indicates that moisture removal is faster in the top layer compared to the middle and bottom layers. Additionally, the drying curves demonstrate that moisture removal is greater in the 6 mm slices than in the 10 mm slices at a loading density of 53 g/100 cm². Similar findings were reported by Malaikritsanachalee *et al.* (2018) and Lopez *et al.* (2018). However, the difference in the rate of moisture removal between the two thicknesses at a loading density of 107 g/100 cm² is minimal. A probable reason for this observation is the weather conditions on the day of drying.

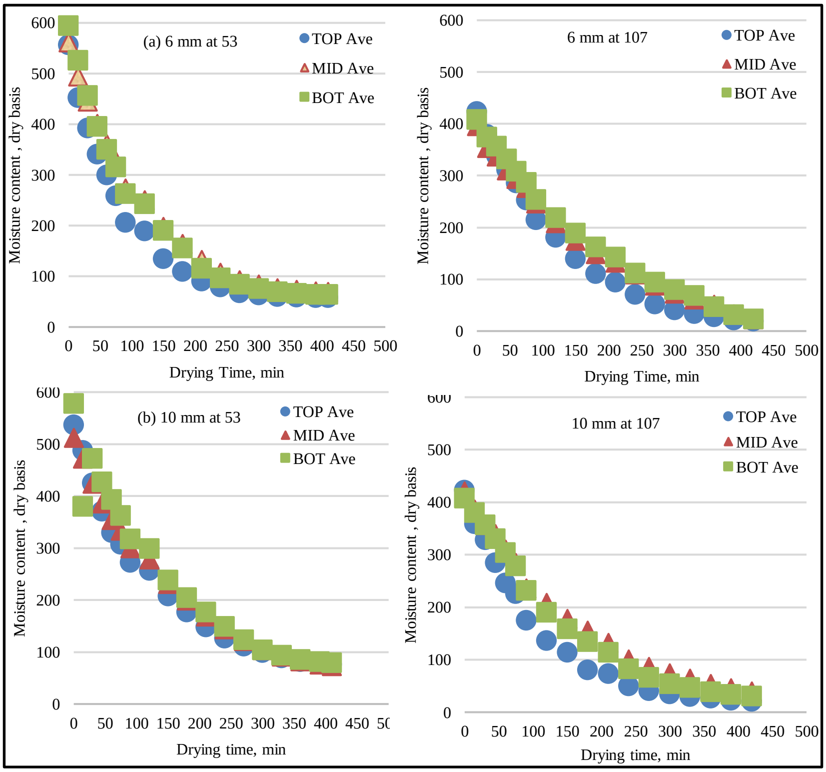

Figure 11. Drying characteristics of dried pineapple slices: 6 mm (a); 10 mm (b) [left figure is at loading density of 53 g/100 cm^2, right figure is at loading density of 107 g/100 cm^2.]

3.3.6 Drying Rate Characteristics of Pineapple Slices

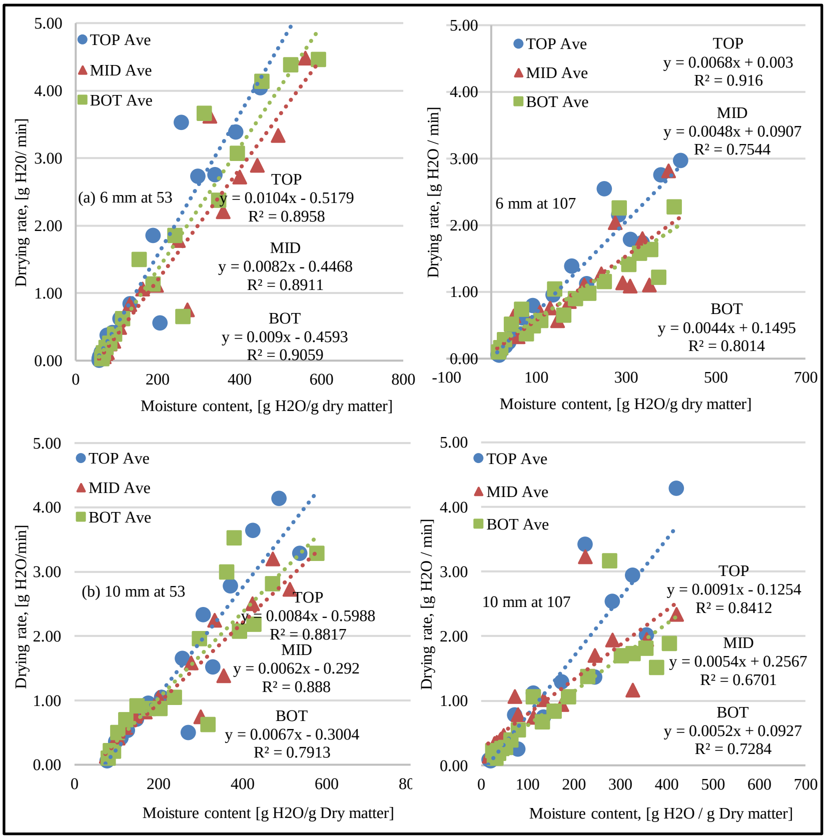

Figure 12. Drying rate characteristics of dried pineapple slices: 6 mm (a); 10 mm (b) [left figure is at loading density of 53 g/100 cm^2, right figure is at loading density of 107 g/100 cm^2.]

The drying rate curves for the two pineapple slice thicknesses at different tray locations and loading densities are shown in Figure 12. These figures illustrate the changes in the rate of moisture removal relative to the moisture content of the samples. The results indicate that the drying of pineapple slices exhibits only one falling rate period. Similar findings were reported by Ramallo and Mascheroni (2013) in their study on the drying of pineapple slices. Linear regression lines were fitted to the drying rate curves to confirm that the drying rate characteristics exhibit the falling rate feature. The equations of the regression lines and the coefficient of determination (R^2) are also presented. As shown in the figure, the slope of the fitted lines ranged from 0.0044 to

0.0091 across all treatments. The slopes for sweetened pineapple slices located in the top layer were observed to be higher than those in the middle and bottom layers. This observation holds true for all samples across both loading densities. This phenomenon can be explained by the reduction of moisture in the pineapple slices due to partial dehydration. The immersion of the slices in the osmotic sucrose solution results in two simultaneous crossflows: a water outflow from the food to the solution and a solute inflow from the solution into the food (Hough *et al.*, 1993; Kumar *et al.*, 2012; Raoult-Wack *et al.*, 1994; Spiazzi and Mascheroni, 1997). Results from the statistical analysis on the drying rate constants shown in Table 4 revealed that both tray location and loading density are significantly different among treatments, as the P-values from the analysis are below 0.05. However, the thickness of the samples was not found to be statistically different. This suggests that the developed solar dryer-roaster can accommodate both slice thicknesses without variation in the rate of moisture removal. Tukey's analysis also indicated a difference in the means under the various tray locations. The drying rate constants of the samples in the top layer are statistically different from those situated in the middle and bottom layers; however, the means for samples located in the bottom and middle layers were not found to be significantly different.

Table 4. Analysis of variance on the value of the regression coefficient on the drying rate of pineapple slices

Source	DF	Adj SS	Adj MS	F-Value	P-Value
Location	2	0.000066	0.000033	23.571	0.0000006
Thickness, mm	1	0.000062	0.000062	43.843	0.0000002
Loading density, g/cm^2	1	0.000005	0.000005	3.496	0.0709912
Error	31	0.000044	0.000001		
Lack-of-Fit	7	0.000031	0.000004	8.322	0.0000366
Pure Error	24	0.000013	0.000001		
Total	35	0.000176			

4. Conclusion and Recommendation

In this study, a newly designed hybridized solar dryer with several solar reflectors was investigated for drying various agricultural commodities, including green Cardaba bananas, ripe mangoes, and ripe pineapples. The new solar dryer-roaster design was used to explore the drying kinetics of the slices under different loading densities, tray locations, and slice thicknesses. The drying characteristics and drying rate constants of the dried samples were analyzed.

The highest drying rates were observed for all samples located in the top layer, which is expected given that the temperature at this location was the highest among all tray positions. The rate of drying also fluctuated due to variations in solar insolation, which affected the temperature distribution within the drying chamber.

During the first falling rate period, the moisture removal rate in all samples was not influenced by the thickness of the slices. This suggests that under the same drying conditions studied, the new dryer design can accommodate both slice thicknesses for all three commodity types without any significant differences.

However, the drying rates of all sample slices were influenced by both loading density and tray location. For optimal drying, samples should be sliced thinner, and the drying trays should be placed in the top section of the drying chamber.

5. Acknowledgement

This publication resulted, in part, from research supported by the Department of Science and Technology (DOST), a DOST-funded project that is co-supported by the University of Science and Technology of Southern Philippines (USTP). We sincerely acknowledge and appreciate DOST and USTP for their financial support of this project. The content presented herein is solely the responsibility of the authors and does not necessarily reflect the official views of DOST or USTP.

6. References

Abd El-Wahhab, G.G., Sayed, H.A.A., Abdelhamid, M.A., Zaghlool, A., Nasr, A., Nagib, A., Bourouah, M., Abd-ElGawad, A.M., Rashad, Y.M., Hafez, M., & Taha, I.M. (2023). Effect of pre-treatments on the qualities of banana dried by two different drying methods. Sustainability. 15(20):15112. https://doi.org/10.3390/su152015112

Asrey, R., Sharma, S., Barman, K., Prajapati, U., Negi, N., & Meena, N. (2023). Biological and postharvest interventions to manage the ethylene in fruit: A review. Sustainable Food Technology, 1. doi:10.1039/D3FB00037K

CDO Encyclopedia. (n.d.). Cagayan de Oro 1st public market in Mindanao to use solar power. Accessed online July 30, 2024. https://www.cdopedia.com/cdo-dev/cagayan-de-oro-1st-public-market-mindanao-use-solar-power

Dereje, B., Abera, S., & Yildiz, F. (2020). Effect of pretreatments and drying methods on the quality of dried mango (*Mangifera indica L.*) slices. Cogent Food & Agriculture, 6(1). https://doi.org/10.1080/23311932.2020.1747961

Elhesain, M., Mustafa, W., Abdalla, M., & Bukhari, M. (2023). Comparative study between different drying methods using thin-layers of mango slices (*Mangifera indica L.*). Food Technology Research Journal, 2(3), 101-110. doi: 10.21608/ftrj.2023.334165

Espinoza-Espinoza, L.A., Juárez-Ojeda, C.E., Ruiz-Flores, L.A., Moreno-Quispe L. A., Anaya-Palacios, M.S., & Cárdenas-Quintana, H. (2023). Influence of convection drying with hot air on the physicochemical and phytochemical properties of green banana flour (*Musa cavendish*). Front. Sustain. Food Syst. 7:1204349. doi: 10.3389/fsufs.2023.1204349

Gerance, A.A. (2023). Assessing postharvest handling practices and reframing losses through a systems approach: the case of "queen" pineapple value chain in Camarines Norte, Philippines. Agriculture, economy and politics. ⟨dumas-04501483⟩ Accessed June 20, 2024.

Gilago, M.C., Mugi, V.R., Chandramohan, V.P., & Suresh, S. (2023). Evaluating the performance of an indirect solar dryer and drying parameters of pineapple: comparing natural and forced convection. Journal of Thermal Analysis and Calorimetry. 148, 3701–3709. https://doi.org/10.1007/s10973-023-11955-2

Gilago, M. & Chandramohan, V.P. (2023). Study of drying parameters of pineapple and performance of indirect solar dryer supported with thermal energy storage: Comparing passive and active modes. Journal of Energy Storage. 61. 106810. 10.1016/j.est.2023.106810.

Hough, G., Chirife, J., & Marini, C. (1993). A simple model for osmotic dehydration of apples. LWT-Food Science and Technology, 26(2), 151-156.

Jerusalem, J. (2024). Local firm promotes renewable energy in Mindanao for 13 years. Philippine News Agency. https://www.pna.gov.ph/articles/1147627

Kumar, V., Kumar, G., & Sharma, P.D. (2012). Osmotic dehydration of litchi pulp as a pretreatment for drying processes. Agricultural Engineering International: CIGR Journal, 14(3), 146-151.

Liang, K., Zhang, H., Chen, H., Gao, D., & Liu, Y. (2021). Design and test of an annular fresnel solar concentrator to obtain a high-concentration solar energy flux. Energy 214, 118947. doi:10.1016/j.energy.2020.118947

López-Cerino, I., López-Cruz, L.I., Nagle, M., Mahayothee, B., & Müller, J. (2018). Thin layer drying of Pineapple (Ananas comosus, L.). Ingeniería, investigación y tecnología.

Lytefire Inc. (2024). Lytefire PRO All-in-One. https://lytefire.com/all-in-one. Accessed June 19, 2024

Malaikritsanachalee, P., Choosri, W., & Choosri, T. (2018). Study on kinetics of flow characteristics in hot air drying of pineapple. Food Sci Biotechnol. 2018 Mar 28;27(4):1047-1055. doi: 10.1007/s10068-018-0357-6. Erratum in: Food Sci Biotechnol. 2018 Jun 12;27(4):1245. PMID: 30263834; PMCID: PMC6085240.

Minitab, LLC. (2021). Minitab. Retrieved from https://www.minitab.com

Mohammed, S., Edna, M., & Siraj, K. (2020). The effect of traditional and improved solar drying methods on the sensory quality and nutritional composition of fruits: A case of mangoes and pineapples. Heliyon 6, e04163.

Mohana, Y., Mohanapriya, R., Anukiruthika, T., Yoha, K.S., Moses, J.A., & Anandharamakrishnan, C. (2020). Solar dryers for food applications: concepts, designs, and recent advances, Solar Energy, Volume 208, ISSN 0038-092X.

Mopera, L.E. (2016). Food loss in the food value chain: the Philippine agriculture scenario, Journal of Developments in Sustainable Agriculture. 11(1), 8-16.

Mugodo, K., & Workneh, T.S. (2021). The kinetics of thin-layer drying and modelling for mango slices and the influence of differing hot-air drying methods on quality. *Heliyon*, *7*.

Mustayen, A.G.M.B., Mekhilef, S., & Saidur, R. (2014). Performance study of different solar dryers: A review. Renewable and sustainable energy reviews, volume 34, ISSN 1364-0321.

PSAX-SR-2020-13. Philippine Statistics Authority Region 10. Highlights of Selected Major Crops Production in Northern Mindanao. (First Quarter 2020)

Pech, J.C., Bouzayen, M., & Latché, A. (2008). Climacteric fruit ripening: Ethylene-dependent and independent regulation of ripening pathways in melon fruit. Plant Science, 175(1), 114-120. doi:https://doi.org/10.1016/j.plantsci.2008.01.003

Pekke, M.A., Pan, Z.L., Atungulu, G.G., Smith, G., & Thompson, J.F. (2013). Drying characteristics and quality of bananas under infrared radiation heating. Int J Agric & Biol Eng, 2013; 6(3): 58－70.

Pirasteh, G., Saidur, R., Rahman, S.M.A., & Rahim, N.A. (2014). A review on development of solar drying applications. Renewable and Sustainable Energy Reviews 31, 133-148. DOI: 10.1016/j.rser.2013.11.052

Phyu, T.A., Soe, T.T. Theingi, M., & Kyaw, P.N.D. (2024). Influenced by different drying methods on physico-chemical properties of dried mango slices (*cv. Yinkwae mango*) (*Mangifera indica L*.). Acta Scientific Nutritional Health 8(3), 22-26.

Raoult-Wack, A.L., Rios, G., Saurel, R., Giroux, F., & Guilbert, S. (1994). Modeling of dewatering and impregnation soaking process (osmotic dehydration). Food Research International, 27(2), 207-209.

Ramallo, L. & Mascheroni, R. (2013). Effect of shrinkage on prediction accuracy of the water diffusion model for pineapple drying. Journal of Food Process Engineering. 36. 10.1111/j.1745-4530.2011.00654.x.

Rani, P. & Tripathy, P. (2022). Investigating shrinkage corrected drying characteristics, rehydration, color profile and microstructural evolution during solar drying of pineapple slices. Journal of Food Process Engineering. 45. 10.1111/jfpe.14036.

Salazar-Camacho, N.A., Sanchez-Echeverri, L.A., Fonseca, F.J., Falguera, V., Castro-Bocanegra, D., & Tovar-Perilla, N.J. (2022). Mango (*Mangifera indica L.*) dehydration as a women entrepreneurship alternative in vulnerable communities. Sustainability 2022, 14, 1548. https://doi.org/10.3390/su14031548

Sacilik, K. (2007). Effect of drying methods on thin-layer drying characteristics of hull-less seed pumpkin (*Cucurbita pepo L.*). Journal of Food Engineering, 79, 23–30. https://doi.org/10.1016/j.jfoodeng.2006.01.023

Silva, Á.G.F.D., Cruz, R.R.P., Moreira, W.G., Pereira, M.A.F., Silva, A.S.A., Costa, F.B.D., Nascimento, A.M.D., Souza, P.A.D., Timoteo, A.L.D. S., & Ribeiro, W.S. (2022). Solar drying of 'Prata' bananas. Food Science and Technology, 42, e75021.

Spiazzi, E. & Mascheroni, R. (1997). Mass transfer model for osmotic dehydration of fruits and vegetables—I. Development of the simulation model. Journal of Food Engineering, 34(4), 387-410.

Tan, D.L.S., Perez, J.H., & Diamante, L.M. (2006). Thin-layer drying of cassava chips and grates, Acta Hort. (International Society for Horticultural Science), 2006, 703, p. 233-240.

Thao, B.T.T., Thanh Hung, P., Lai, N.D., Tran, T.Y.N., Nguyen, N.Q., Pham, T.N., Truc Tran, T., Giang Bach, L., & Dao, T.P. (2024). Application of heat pump drying technology to produce dried mango products from Tu Quy mango (*Mangifera india L.*), Vietnam, on a pilot scale. Front. Sustain. Food Syst. 8:1204303. doi: 10.3389/fsufs.2024.1204303

Xiao, J., Zheng, H., Jin, R., Shen, L., Wang, G., & Ma, X. (2021). Experimental investigation of a bubbling humidification-dehumidification desalination system directly heated by cylindrical Fresnel lens solar concentrator. Sol. Energy 220, 873–881. doi:10.1016/j.solener.2021.04.006

Yan, Z., Gallagher, M.J.S., & Oliveira, F.A.R. (2008). Shrinkage and porosity of banana, pineapple and mango slices during air-drying. Journal of Food Engineering, 84(3), 430–440. https://doi.org/info:doi/.

Zhang, J., Cheng, D., Wang, B., Khan, I., & Ni, Y. (2017). Ethylene control technologies in extending postharvest shelf life of climacteric fruit. Journal of Agricultural and Food Chemistry, 65(34), 7308-7319. doi:10.1021/acs.jafc.7b02616